第35卷第10期
2007年10月

华南理工大学学报(自然科学版)
Journal of South China University of Technology
(Natural Science Edition)

Vol. 35 No. 10
October 2007

Article ID: 1000-565X(2007)10-0020-06

Design of Power Conditioning System for Fuel Cell Power Plant*

Huang Shi-sheng Tang Zhao-yang Wang Zhen-min Chen Yi-ting

(School of Mechanical Engineering, South China Univ. of Tech., Guangzhou 510640, Guangdong, China,)

Abstract: The power conditioning system of a fuel cell power plant is very important to the reliability and efficiency of the power plant system as well as to the quality of the output waveform. In this paper, the optimized cooperation between the main circuit structure of the power conditioner and the fuel cell parameters is investigated by simulation and experiment, and the law of designing efficient main circuit for the power conditioning system is proposed. By investigating the mathematical model of the inverter system, some guidance is provided for the inverter output waveform control. A digital intelligent control system with good practicability, high performance and low cost is then designed, in which the output waveform control is emphasized. Moreover, the waveform control scheme based on the sliding-mode control policy is investigated, and is then testified by experiments. It is found that the proposed system satisfies the requirements of the power plant, and possesses good reliability, high output waveform quality and great efficiency.

Key words: fuel cell power plant; power conditioning system; inverter; waveform control; sliding-mode control

CLC number: TM464; TM76 **Document code**: A

0 Introduction

Fuel cell is called the equipment using chemist energy to generate electricity or molecule to generate electricity that generates electricity by converting the chemical energy of fuel into electric power directly. So that it is of high ratio of energy converting and almost has no negative influence on the environment. As the energy source is lacking and the environmental pollution is severe nowadays, it is a favor to use fuel cell power plants to substitute thermo-electric plants. The output voltage of fuel cell, usually low, is a variable determined by working temperature, pressure and output current. It is necessary to improve the performance of output voltage of fuel cell by converting it into high and stable voltage. Moreover, fuel cell supplies direct current, but alternating current is needed in most applications. Thus, an inverter is needed to convert DC into AC.

A fuel cell power plant consists of the fuel subsystem, the cell subsystem and the power conditioning system (PCS). The function of PCS is to convert the output DC of the fuel cell into a three-phase AC with stable voltage and frequency[1-4].

Though fuel cell has many advantages, it is still not popularized due to its high cost of building and running. In China, the study on the application technologies of fuel cell is in junior stage at present. The development of PCS with high conversion efficiency, high quality, high reliability and low cost is important for the generalization of the application of fuel cell power plants. In this paper, the main circuit and digital controller of PCS are studied.

Received date: March 2, 2007

* **Foundation item**: Supported by a grant from the Major Programs of Science and Technology Foundation of Guangdong Province Industry (124B2041570)

Biography: Huang Shi-sheng (born in 1938), male, professor, doctoral supervisor, mainly researches on digital power source and inverter power supply for welding. Email: sshuang@scut.edu.cn

1 Main Circuit of PCS

There are two classes of main circuits of PCS, one is an inverter connecting fuel cell directly, and the other is an inverter appended some circuits to ascend and steady the voltage, for example a boost. In this paper, two different designs of the main circuit structure of fuel cell power plant are proposed[2,6]. By modeling and simulating the main circuits with the Matlab software, the suitable one is chosen from the two schemes based on the analysis of simulation results.

1.1 Fuel Cell Connecting Inverter Through a Boost

The work voltage of IGBT (Insulated-Gate Bipolar Tyansistor) can be decided by the output voltage of fuel cell and boost. By considering the voltage concussion in the course of switching, the highest work voltage of switch should be higher than the calculated value.

After the work voltage is decided, the work current can be expressed as

$$I=\frac{S}{U}\lambda \tag{1}$$

where S is the total output power of the power plant, λ is the safety factor, and U is the output voltage of the inverter.

The output waveform is better when the work speed of switch is higher. But on the other hand, more switch times bring more power wasting and more heat, which should be considered concordantly.

In a boost-inverter circuit, the output voltage of the boost is chosen according to the output voltage of the inverter and the voltage converter efficiency of the inverter. It is expressed as

$$U=\frac{\sqrt{3}}{2}U_{\mathrm{D}}\times\alpha \tag{2}$$

Where U_{D} is the input voltage of the inverter, and α is the degree of modulation.

When an ideal boost is working under continuous pattern, its voltage plus factor is expressed as

$$M=\frac{1}{D} \tag{3}$$

where M is the voltage plus factor and D is the break-off occupying ratio of power switch.

In practice, the components of circuit have parasitical parameters. By considering the parasitical parameters of R_L and R_C, the voltage plus factor is expressed as

$$M=\frac{1}{D}\left[\frac{D^2R}{R'}\right] \tag{4}$$

where $R'=R_L+(R/R_C)D+\dfrac{R^2D_1^2}{R+R_C}$ and D_1 is the switch-on occupying ratio.

Thus, the voltage plus of an applied boost is finite, and it should be always working in the range of larger voltage plus.

High-power boost should be designed to work under continuous current mode. So that, the parameters of components can be calculated as

$$L_C=\frac{V_oT_s}{2I_{o,\min}}D_{\min}(1-D_{\min})^2 \tag{5}$$

$$I_{L(\mathrm{rms})}=\frac{V_o}{R}\left[\left(\frac{1}{1-D_1}\right)^2+\frac{1}{3}\left(\frac{1}{2\tau_L}\right)^2D_1(1-D_1)\right]^{\frac{1}{2}} \tag{6}$$

where L_C is the critical value of inductance, V_o is the output voltage of the boost, T_s is the cycle of the switch, $I_{o,\min}$ is the minimum output current, $D_{\min}$ is the minimum break-off occupying ratio of power switch, $I_{L(\mathrm{rms})}$ is the virtual value current of inductance, and τ_L is the critical time factor.

Capacitance when boost working under limited voltage ripple is expressed as

$$C=\frac{D_1T_s}{\Delta V_o}I_o \tag{7}$$

where ΔV_o is the fluctuation of output voltage.

And its ability of passing ripple current $I_{C(\mathrm{rms})}$ is expressed as

$$I_{C(\mathrm{rms})}=\frac{V_o}{R}\sqrt{\frac{D_1}{1-D_1}+\frac{D_1}{12}\left[\frac{(1-D_1)RT_s}{L}\right]^2} \tag{8}$$

A RCD (Resistor-Capacitor-Diode) protection snubber circuit is adopted to protect IGBT, which is designed as

$$C=\frac{I_C(t_r+t_f)}{V_{\mathrm{CE}}},\quad R=\frac{t_{\mathrm{on}}}{3C},\quad P_R=\frac{1}{2}CV_{\mathrm{CE}}^2f \tag{9}$$

where t_r is the turning-on time of switch, t_f is the break-off time of switch, and V_{CE} is the working voltage of switch.

When the output voltage of fuel cell is 300 V DC, the power plant output is three-phase 220 V and 50 Hz sine wave AC, and the rated output power is 50 kW, the main circuit of boost-inverter structure is designed. Then Matlab software is used to model and simulate it. Fig. 1 is the model of boost-inverter system and Fig.2 is the simulated curve.

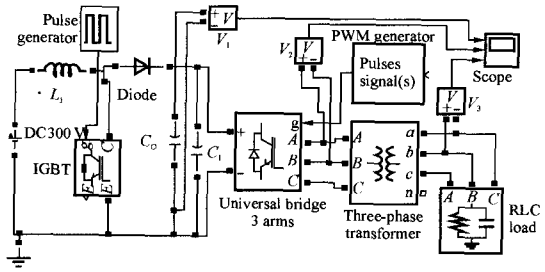

Fig. 1 Model of boost-inverter system

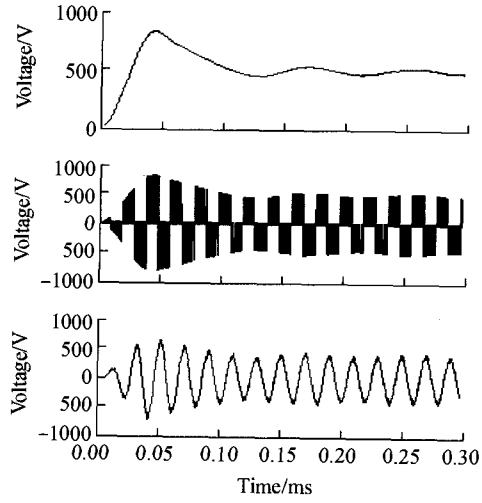

Fig. 2 Simulation results of boost-inverter system

1.2 Fuel Cell Connecting Inverter Directly

When a fuel cell is linked with the inverter and the output filter directly, the system has fewer components. Thus, the ratio of component failure is smaller and the system has higher reliability. The choice of IGBT parameters can consult Eq.(1), and its voltage concussion protection circuit adopts RCD snubber. The critical capacitance C_s, the critical resistance R_s and the power of critical resistance P_{R_s} are expressed as

$$\begin{cases} C_s = I^2 \dfrac{L}{\Delta U^2},\ R_s \leqslant \dfrac{1}{2.3 \times C_s \times f_s} \\ P_{R_s} = C_s \Delta U^2 f_s / 2 \end{cases} \tag{10}$$

where I is the working current, ΔU is the concussion voltage, L is the wire parasitic inductance, and f_s is the working frequency of switch.

Under the condition that the output voltage of fuel cell is 300 V DC, the power plant output is three-phase 220 V and 50 Hz sine wave AC, and the rated output power is 50 kW, the main circuit of fuel cell directly connecting the inverter is designed. Then, according to the parameters of the components, simulation model is established by using Matlab software. Fig.3 is the model and Fig. 4 is the simulation results.

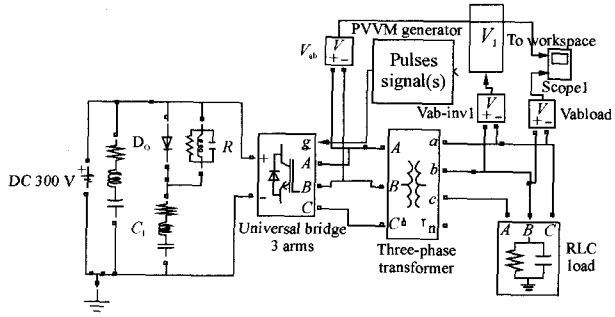

Fig. 3 Model of the system that inverter directly connects to fuel cell

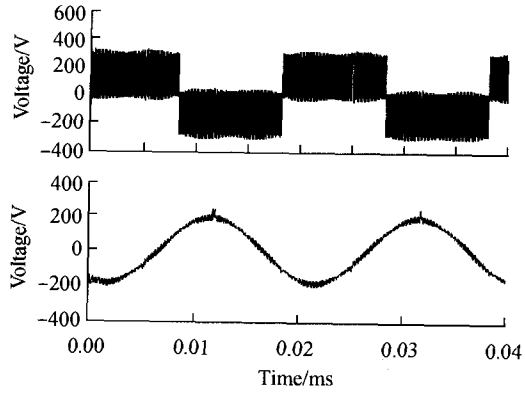

Fig. 4 Simulation results of the system that inverter directly connects to fuel cell

By comparing the simulation results, it can be found that when the output voltage of fuel cell is 300 V, the power loss ratio of the main circuit linking fuel cell via an inverter directly is smaller than that of the main circuit of boost-inverter system.

2 Digital Control of PCS

The digital control system consists of the hardware and the software. The former is composed of the sampling module, the embedded microcontroller and the IGBT driver. The latter is developed using embedded

C language on the integration development system CCS2.2.

2.1 Hardware of the Controller

2.1.1 Embedded Processor

High-performance DSP (Digital Signal Processing) microprocessor TMS320F2812 of TI is adopted as the core of the embedded controller. It has many digital I/O and useful on-chip peripherals. The embedded control system is illustrated in Fig. 5, which possesses high running speed, large memory space and flexible structure.

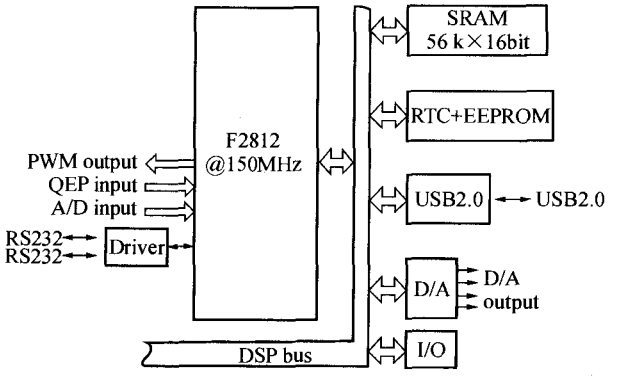

Fig. 5 Diagram of embedded DSP control system

2.1.2 Sampling Module

The sampling module provides the embedded control system with feedback control signal. A real-time feedback signal without distortion is required for a control system to work stably. It consists of the sensor, the filter and the AD converter. Here, the sensor adopts Hall components to fulfilling the real-time AC signal collection.

The filter can adopt hardware filter and digital filter. The hardware filter adopts LC low-pass filter. The F2812DSP AD module has an input voltage ranging in about 0 ~ 3 V. Therefore, the sensor output signal voltage must be limited and moved to the range of 0 ~ 3 V. To protect the peripherals from over voltage, a circuit is used to limit the signal voltage before the signal enters AD converter module. And, at last a digital filter is needed to restrain the noise from entering into the feed back signal.

2.2 Software and Control Arithmetic

The embedded DSP control software should have the functions such as the PWM arithmetic and drive, the safety running control for PCS and the output waveform control for power plant. The flow chart of system software is illustrated in Fig. 6.

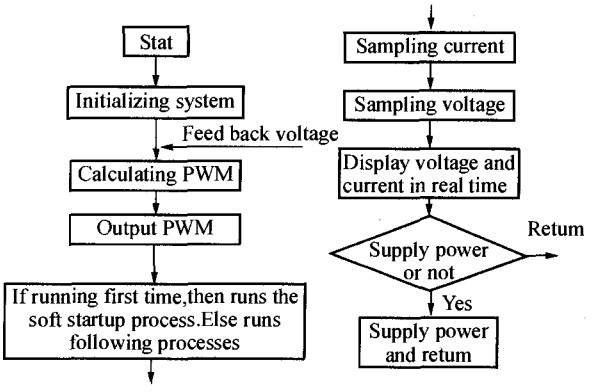

Fig. 6 Flow chart of system control software

Among the control functions, the waveform quality is the main target for the performance of power conditioner system. And the waveform control in embedded DSP control software is key and difficult. In this paper, sliding mode control policy is adopted, the advantage of which is that it is not sensitive to structure parameter change and external disturbance. It has strong robustness and inherent switch characteristics. So that, it is particularly suitable for the closed-loop control of power electronic system[7-10]. Analysis and study of sliding mode control of power conditioning system's output waveform will be carried out in the following sections.

In Fig. 7, there is a neutral, and the phase voltages and currents of the three phases of inverter are independent upon each other. So that, there are six independent variables in the system. By taking the output voltages of inverter $u_{o,a}$, $u_{o,b}$, $u_{o,c}$ and inductance currents $i_{L,a}$, $i_{L,b}$, $i_{L,c}$ as state variables, the state space equations of the three-phase inverter can be formulated. Every equation relates only parameters of one phase, and the equations can be decoupled. Thus, the three-phase output can be controlled separately, and a system can be regarded as three single-phase inverter systems with 120-degree phase differences among them. In order to simplify the analysis, one can choose only one phase to study, and the parameters of the other two phases are the same. Based on the current and voltage laws of Kirchhoff, equations can be written as

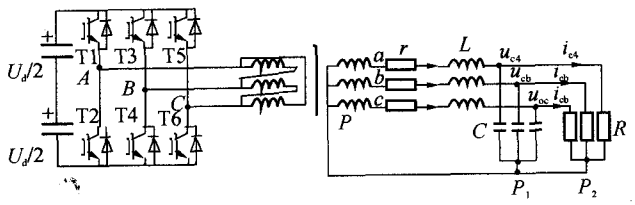

Fig. 7 Circuit of three-phase inverter system

$$\begin{cases} C\dfrac{\mathrm{d}u_{o,a}}{\mathrm{d}t} = i_{L,a} - i_{o,a} \\ u_A - u_p = L\dfrac{\mathrm{d}I_{L,a}}{\mathrm{d}t} + ri_{L,a} + u_{o,u} \end{cases} \tag{11}$$

where u_A is the output voltage of phase A of the inverter, u_p is the grounding voltage, L is the inductance of the inductor, C is the capacitance of the capacitor. If

$$u_{1,a} = u_A - u_p,\ A_0 = \begin{bmatrix} -\dfrac{R}{C} & \dfrac{1}{C} \\ -\dfrac{1}{L} & -\dfrac{r}{L} \end{bmatrix},\ B_0 = \begin{bmatrix} 0 \\ \dfrac{1}{L} \end{bmatrix},$$

Eq.(11) can be expressed as

$$\begin{bmatrix} \dot{u}_{o,a} \\ \dot{i}_{L,a} \end{bmatrix} = \begin{bmatrix} -\dfrac{R}{C} & \dfrac{1}{C} \\ -\dfrac{1}{L} & -\dfrac{r}{L} \end{bmatrix} \begin{bmatrix} u_{o,a} \\ i_{L,a} \end{bmatrix} + \begin{bmatrix} 0 \\ \dfrac{1}{L} \end{bmatrix} [u_{1,a}] = A_0 \begin{bmatrix} u_{o,a} \\ i_{L,a} \end{bmatrix} + B_0 [u_{1,a}] \tag{12}$$

In discrete time, the state equation is expressed as

$$x(k+1) = Ax(k) + Bu(k) \tag{13}$$

Let $r(k)$ to denote the voltage instruction, $\mathrm{d}r(k)$ to denote the change rate of voltage instruction and $R = [r(k), \mathrm{d}r(k)]$, $R_1 = [r(k+1), \mathrm{d}r(k+1)]$, there is

$$r(k+1) = 2r(k) - (k-1),$$
$$\mathrm{d}r(k+1) = 2\mathrm{d}r(k) - \mathrm{d}r(k-1) \tag{14}$$

The switching function $s(k)$ can be expressed as

$$s(k) = C_e(R - x(k)) \tag{15}$$

where $C_e = [c_p, 1]$, c_p is parameter of the controller.

It can thus be deduced that

$$s(k+1) = C_e(R_1 - x(k+1)) = C_eR_1 - C_eAx(k) - C_eBu(k).$$

The control law is expressed as

$$u(k) = (C_eB)^{-1}(C_eR_1 - C_eAx(k) - s(k+1)) \tag{16}$$

The discrete reaching law based on exponential reaching law is expressed as

$$s(k+1) = s(k) + \mathrm{T}(-\varepsilon \mathrm{sgn}(s(k)) - qs(k)) \tag{17}$$

Deduced from equations (16) and (17), the control law based on exponential reaching law is expressed as

$$u(k) = (C_eB)^{-1}(C_eR_1 - C_eAx(k) - s(k) - \mathrm{d}s(k)) \tag{18}$$

where $\mathrm{d}s(k) = -\varepsilon T\mathrm{sgn}s(k) - qTs(k)$.

3 Simulation and Experiments

The parameters and performance requirements of power plant are as follows: the fuel cell output is 300 V DC, the power plant outputs three-phase 400 V and 50 Hz sine wave AC, and the rating output power of power plant is 50 kW.

By analyzing the simulation results of the model, the inverter circuit directly linking to the fuel cell is selected as the main circuit. The IGBT adopts 450-ampere work current under 80 Celsius degrees, and the work voltage is 1 200 V. The switch speed is 6 kHz. The capacitance of the output filter is 30 μF and the inductance is 700 μH. The equivalent inner resistance of the system is 0.1 Ω, and the experiment load is 20 kW resistance load. The sampling frequency of the control system is 48 kHz, and the discrete time state is expressed as

$$x(k+1) = Ax(k) + Bu(k),$$

where $A = \begin{bmatrix} 0 & 33333 \\ -1428 & -142.8 \end{bmatrix}$, $B = \begin{bmatrix} -33333 \\ 1428 \end{bmatrix}$.

The parameters of the controller are $c_p = 10$, $\varepsilon = 5$ and $q = 25$. The original state assumes as $[-0.5 \quad -0.5]$.

Experiments on the designed PCS are carried out. The results are shown in Fig. 8.

Fig. 8(a) is the voltage curve of phase A electricity when the three phases of electricity are fully loaded. Fig. 8(b) is the voltage curve of phase B electricity when phase B electricity is fully loaded and the other two phases of electricity are emptily loaded. Fig. 8(c) is the voltage curve of phase C electricity when phase C electricity is emptily loaded and the other two phases of electricity are fully loaded.

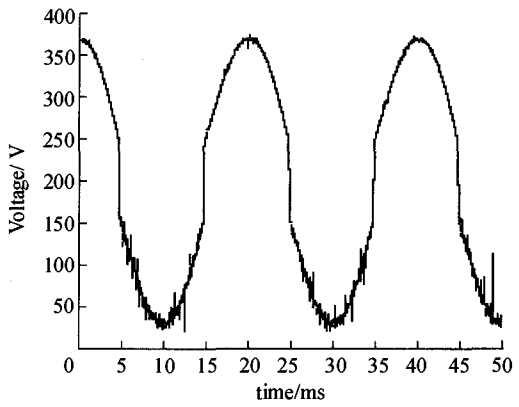

(a) Voltage curve of phase *A* electricity

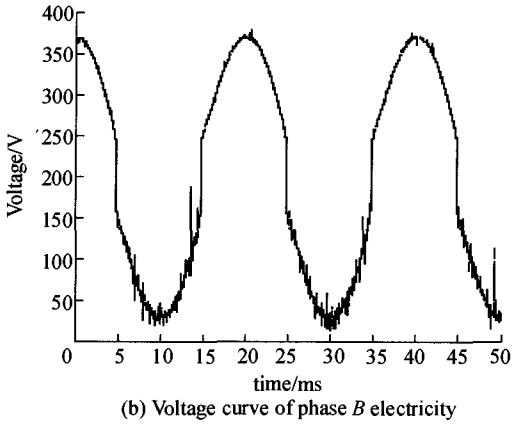

(b) Voltage curve of phase *B* electricity

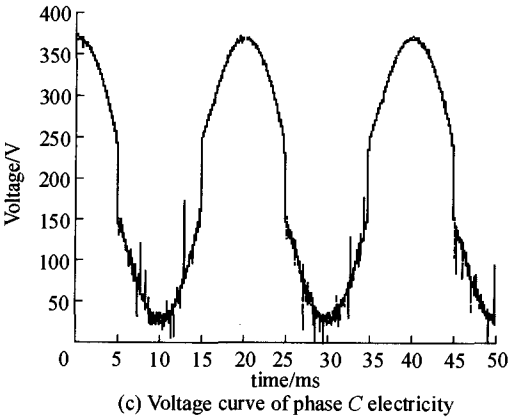

(c) Voltage curve of phase *C* electricity

Fig. 8 Waveforms of the output voltage of power plant

4 Conclusion

The PCS for fuel cell power plant designed in this paper adopts high-efficiency power switch IGBT.

Efficient and stable main circuit is the base of a good PCS. When the fuel cell has low output voltage, taking measures to ascend and stabilize DC voltage is helpful to improve the working performance of system. In this paper, the fuel cell is of an output voltage of 300 V, when considering the power wasting of booster itself , the circuit connecting an inverter with fuel cell directly will has better efficiency.

The digital controller uses a DSP microprocessor as the core processor, which can adopt intelligent control policy conveniently. Experimental results indicate that the adopted sliding-mode control for waveform control works well. The PCS works stably and the fuel cell power plant output voltage waveform is good.

References:

[1] [日]电气学会. 燃料电池发电 21 世纪系统技术调查专门委员会. 燃料电池技术 [M]. 谢晓峰,范星河,译. 北京:化学工业出版社,2004.

[2] Santi E, Franzoni D, Monti A, et al. A fuel cell based domestic uninterruptible power supply [J]. Applied Power Electronics Conference and Exposition, 2002(1):605-613.

[3] Cheng K W E, Sutanto D, Ho Y L, et al. Exploring the power conditioning system for fuel cell [J]. Power Electronics Specialists Conference, 2001(4):2197-2202.

[4] Xie Li-hua, Su Yan-min. Digital control technic of sinusoidal inverter power source [J]. Power Electronic, 2001, 35(6):52-57.
谢力华,苏彦民. 正弦波逆变电源的数字控制技术 [J]. 电力电子技术,2001,35(6):52-57.

[5] Song Yu-jim, Enjti Prasad N. A high frequency link direct dc-ac converter for residential fuel cell power systems [J]. Power Electronics Specialists Conference, 2004(6): 4755-4761.

[6] Young K D, Utkin V I. A Control engineer's guide to sliding mode control [J]. IEEE Transactions on Control System Technology, 1999, 7(3):328-342.

[7] Zhang Chang-fan, Wang Yao-nan. Sliding mode variable structure aptitude control and its application [J]. Proceedings of the CSEE, 2001, 21(3):27-29.
张昌凡,王耀南. 滑模变结构的智能控制及其应用 [J]. 中国电机工程学报,2001,21(3):27-29.

[8] Gao W B, Wang Y F, Homaifa A. Discrete-time variable structure control systems [J]. IEEE Transactions on Industrial Electronics, 1995, 42(2):117-122.

[9] Tai Tsang-li, Chen Jian-shiang. UPS inverter design using discrete-time-sliding-mode control scheme [J]. IEEE Tramsactions on Industry Electrons, 2002, 49(1):67-75.

[10] Gopinath Rajesh, Kim Sangsun, Hahn Jaehong, et al. Development of a low cost fuel cell inverter system with dsp control [J]. IEEE Fransactions on Power Electronics, 2004, 19(5):1256-1262.

(下转第 48 页)

[18] [苏]M. T. 洛沙克. 硬质合金的强度和寿命 [M]. 黄鹤翥 译. 北京:冶金工业出版社,1990:1-2.
[19] 株洲硬质合金厂. 硬质合金生产 [M]. 北京:冶金工业出版社,1974.
[20] 孙宝琦. 关于 WC-Co 硬质合金的强度和结构问题(Ⅰ) [J]. 稀有金属与硬质合金,2004(3):47-59.
Sun Bao-qi. Study of strength and structure of WC-Co hard alloy (Ⅰ) [J]. Rare Metals and Cemented Carbides,2004(3):47-59.
[21] 孙宝琦. 关于 WC-Co 硬质合金的强度和结构问题(Ⅱ) [J]. 稀有金属与硬质合金,2004(6):29-34.
Sun Bao-qi. Study of strength and structure of WC-Co hard alloy (Ⅱ) [J]. Rare Metals and Cemented Carbides,2004(6):29-34.

Review of High-Speed & Precise Progressive Dies of IT Products

Ruan Feng Huang Zhen-yuan Zhou Chi Wang Bo
(School of Mechanical Engineering, South China Univ. of Tech., Guangzhou 510640, Guangdong, China)

Abstract: This paper investigates both the intelligent design technology and the fracture failure of high-speed & precise progressive dies of IT products. In the investigation, the methods of fuzzy processing, fuzzy clustering and attribute reduction are adopted to make the tacit knowledge of stamping die design explicit, thus achieving the knowledge mining from the design of precise progressive dies. The results of microscopic test show that, in the fracture section, the WC grains are inhomogeneous in size, and the Co content is less than that of the initial carbide material. Analytical results indicate that the fracture failure of the die occurs possibly because the inhomogeneity of WC grains reduces the hardness and wear resistance of the carbide material, and because the Co loss weakens the strength of the material.

Key words: IT product; high-speed & precise progressive die; knowledge mining; fracture

责任编辑: 张君晓

(上接第 25 页)

燃料电池电站功率调节系统的设计*

黄石生 唐朝阳 王振民 陈意庭
(华南理工大学 机械工程学院, 广东 广州 510640)

摘 要: 燃料电池电站功率调节系统对整个电站系统工作的可靠性、效率和输出波形质量有很重要的影响. 文中通过仿真、实验的方式, 研究电路结构与燃料电池参数的优化配合关系, 提出了高效逆变主电路的设计规律. 通过研究逆变系统的数学模型, 为逆变系统输出波形控制技术提供理论依据和指导, 并研制了实用的、高性能和低成本的数字化、智能化控制系统, 其中着重于数字控制系统的逆变器输出波形控制技术. 文中还采用滑模变结构控制策略研究了波形控制技术,并通过实验进行了验证. 结果表明, 文中所提出的设计方案满足了系统功能要求, 并具有良好的可靠性、输出波形质量和较高的转换效率.

关键词: 燃料电池电站; 功率调节系统; 逆变器; 波形控制; 滑模控制
中图分类号: TM464; TM76 **文献标识码**: A
文章编号: 1000-565X(2007)10-0020-06

责任编辑: 张君晓

收稿日期: 2007-03-02
* **基金项目**: 广东省科技工业攻关重大项目(124B2041570)
作者简介: 黄石生(1938-),男,教授,博士生导师,主要从事数字化电源及逆变电源焊接研究. E-mail: sshuang@scut.edu.cn